The histone deacetylase Rpd3 regulates the heterochromatin structure of *Drosophila* telomeres

Giosalba Burgio[1,2], Francesca Cipressa[3], Antonia Maria Rita Ingrassia[1,2], Giovanni Cenci[3,*] and Davide F. V. Corona[1,2,*]

[1]Istituto Telethon Dulbecco, c/o STEMBIO, Viale delle Scienze, Edificio 16, 90128 Palermo, Italy
[2]Università degli Studi di Palermo–Dipartimento di Scienze e Tecnologie Molecolari e Biomolecolari – Sezione di Biologia Cellulare, Viale delle Scienze, Edificio 16, 90128 Palermo, Italy
[3]Dipartimento di Biologia di Base ed Applicata, Università dell'Aquila, 67100 Coppito, L'Aquila, Italy
*Authors for correspondence (giovanni.cenci@cc.univaq.it; dcorona@unipa.it)

Accepted 2 March 2011
Journal of Cell Science 124, 2041-2048

doi:10.1242/jcs.078261

Summary

Telomeres are specialized structures at the end of eukaryotic chromosomes that are required to preserve genome integrity, chromosome stability and nuclear architecture. Telomere maintenance and function are established epigenetically in several eukaryotes. However, the exact chromatin enzymatic modifications regulating telomere homeostasis are poorly understood. In *Drosophila melanogaster*, telomere length and stability are maintained through the retrotransposition of specialized telomeric sequences and by the specific loading of protecting capping proteins, respectively. Here, we show that the loss of the essential and evolutionarily conserved histone deacetylase *Rpd3*, the homolog of mammalian *HDAC1*, causes aberrant telomeric fusions on polytene chromosome ends. Remarkably, these telomere fusion defects are associated with a marked decrease of histone H4 acetylation, as well as an accumulation of heterochromatic epigenetic marks at telomeres, including histone H3K9 trimethylation and the heterochromatic protein HP2. Our work suggests that *Drosophila* telomere structure is epigenetically regulated by the histone deacetylase Rpd3.

Key words: Telomere, Rpd3, Heterochromatin, Histone acetylation, Histone H3K9 trimethylation, HP2

Introduction

Eukaryotic linear chromosomes have evolved special nucleoprotein structures at their ends, the telomeres, which counterbalance the incomplete replication of terminal DNA and protect chromosome termini from fusion events (De Lange, 2005; Ferreira et al., 2004). Telomere structure is conserved in most eukaryotes and, with few exceptions, consists of short repetitive double-stranded G-rich sequences that end in a single-stranded overhang. Telomeric DNA is elongated by telomerase, a specialized reverse transcriptase that adds short DNA repeats by reverse-transcribing the template region of its RNA component (Nugent and Lundblad, 1998). Telomere repeats bind sequence-specific factors, which in turn recruit additional telomeric proteins, forming multiprotein complexes that are crucial for chromosome-end homeostasis. A well-documented example of such terminal complexes is the six-protein complex shelterin that coats human chromosome ends allowing cells to distinguish telomeres from sites of DNA damage (Palm and de Lange, 2008). Telomeric and subtelomeric DNA from different organisms contain histone modifications that are typical of heterochromatin (Blasco, 2007). Interestingly, recent studies have highlighted some of the roles played by chromatin remodelers and covalent modifiers in the establishment of epigenetic marks essential for telomeres structure and function (Altaf et al., 2007).

The model organism *Drosophila melanogaster* lacks telomerase activity and fly chromosome ends do not consist of telomerase-generated simple repeats. *Drosophila* telomeres are elongated by transposition of three different, but related, non-long terminal repeat retrotransposons called *HeT-A*, *TART* and *TAHRE* (Mason et al., 2008). Like their yeast and vertebrate counterparts, fly telomeres are also protected by multiprotein complexes (Cenci et al., 2005; Ciapponi and Cenci, 2008). Interestingly, the elongation of *Drosophila* telomeres is uncoupled from their capping function, as chromosomes ends devoid of retrotransposons can assemble regular telomeres and can be transmitted for many generations. There is also evidence that terminally deleted *Drosophila* chromosomes can be properly capped regardless the sequence of terminal DNA (Cenci et al., 2005; Mason et al., 2008). Thus, *Drosophila* telomere protection relies on sequence-independent epigenetically determined structures.

The remarkable functional similarity between mammalian and fly telomere-protecting mechanisms makes *Drosophila* an excellent model organism to study telomere biology (Cenci et al., 2005). In order to identify factors responsible for the deposition of epigenetics marks required for the establishment and maintenance of telomere structure and function, we conducted a small biased pilot genetic screen scoring for telomere morphology defects on polytene chromosomes. We found that loss of the essential and evolutionary conserved histone deacetylase *Rpd3*, the homolog of mammalian *HDAC1*, causes aberrant telomeric fusions on polytene chromosome ends. Surprisingly, these *Rpd3*-knockdown-induced telomere fusion defects are associated with a marked decrease of histone H4 acetylation, as well as an accumulation of heterochromatic epigenetic marks at telomeres, including histone H3K9 trimethylation and the overloading of the heterochromatic protein HP2. Our work suggests that telomere chromatin structure is regulated by the histone deacetylase Rpd3, providing one of the first insights into the epigenetic determination of telomere organization in higher eukaryotes.

Journal of Cell Science

Results

Loss of the histone deacetylase Rpd3 causes polytene chromosome telomeric fusions

Polytene chromosomes represent a special structural organization of *Drosophila* salivary glands, consisting of polyploid interphase nuclei, which originate by repeated rounds of DNA replication without cell division. *Drosophila* polytene chromosomes have proven to be an invaluable cytogenetic tool to examine chromosome structure and, at the same time, to rapidly assess the genome-wide distribution of chromatin-binding proteins. Indeed, several studies have revealed that the genome-wide distribution of countless structural and regulatory proteins on polytene chromosomes reflects cellular and interphase chromosome physiology occurring in other developmental stages or tissues (Johansen et al., 1999; Stephens et al., 2004). Therefore, we conducted a biased genetic screen on a small group of genes encoding known chromatin remodelers and members of the histone deacetylase family, by searching for telomere morphology defects on polytene chromosomes. As canonical mutations in these genes are embryonic or early-larval lethal, thereby preventing their role in polytene chromatin structure being addressed, we decided to use salivary-gland-specific RNA interference (RNAi), with a classic GAL4::UAS driving system (Steitz et al., 1998), to knockdown gene expression in the corresponding VDRC (Vienna *Drosophila* RNAi Center) lines. To drive UAS-controlled induction of the RNAi in salivary glands we used *eyeless* (*ey*) promoter-mediated GAL4 expression (*eyGAL4*); in addition to the eye imaginal disks, the *eyeless* promoter has been shown to also efficiently drive the expression of GAL4 in salivary glands (Corona et al., 2007).

RNAi-mediated knockdown for some of the genes analyzed led to modest alterations in polytene chromosome structure (data not shown). However, loss of *Sin3A* or *Rpd3* histone deacetylase function on polytene chromosomes (supplementary material Fig. S1A–F), using multiple VDRC lines with no predicted off-target sites, resulted in the formation of apparently elongated chromosome ends that also underwent frequent telomeric fusions (Fig. 1A–E and supplementary material Fig. S1G–J). Interestingly, eye-specific RNAi-mediated knockdown of *Sin3A* or *Rpd3* caused developmental and differentiation defects in adult eyes (supplementary material Fig. S2A–C) confirming a role for the Sin3A–Rpd3 histone deacetylase complex in cell division and proliferation (Ahringer, 2000). However, silencing of *Sin3A* or *Rpd3* in larval neuroblasts, using a *daGAL4* driver (Corona et al., 2007), did not cause telomeric fusions on mitotic chromosomes (supplementary material Fig. S2D–F). Indeed, previous experiments have suggested that the establishment of telomere function in polytene and mitotic chromosomes are similar, although they probably rely on different mechanisms of maintenance and protection (Cenci et al., 2005; Rashkova et al., 2002), thereby explaining why chromosome-end fusions specifically occur only after RNAi-mediated silencing of *Sin3A* or *Rpd3* on interphase polytene chromosomes.

In order to quantify the chromosome-end fusions in *Sin3A* and *Rpd3* RNAi lines, we developed a scoring system to measure the penetrance of telomeric attachments (supplementary material Fig. S3). On the basis of this scoring system, the observed telomeric fusions upon *Sin3A* and *Rpd3* RNAi were not due to independent mutations present in the driving (*eyGAL4*) or *UAS–RNAi* (*UAS-Sin3A-RNAi*; *UAS-Rpd3-RNAi*) lines (Fig. 1F), nor are they indirectly caused by the activation of the RNAi machinery in salivary glands because the overexpression of *Dicer2* (*eyGAL4*; *UAS-Dicer2*) does not cause an increase in telomere fusions when compared with wild-type *Df(1)yw* chromosomes (Fig. 1F) (Dietzl et al., 2007). Our scoring system also revealed that knockdown of the histone deacetylase catalytic subunit encoded by *Rpd3* yielded a higher frequency of telomere fusions when compared with knockdown of *Sin3A* (Fig. 1F). Therefore, to address further the role of the Sin3A–Rpd3 deacetylase complex in telomere

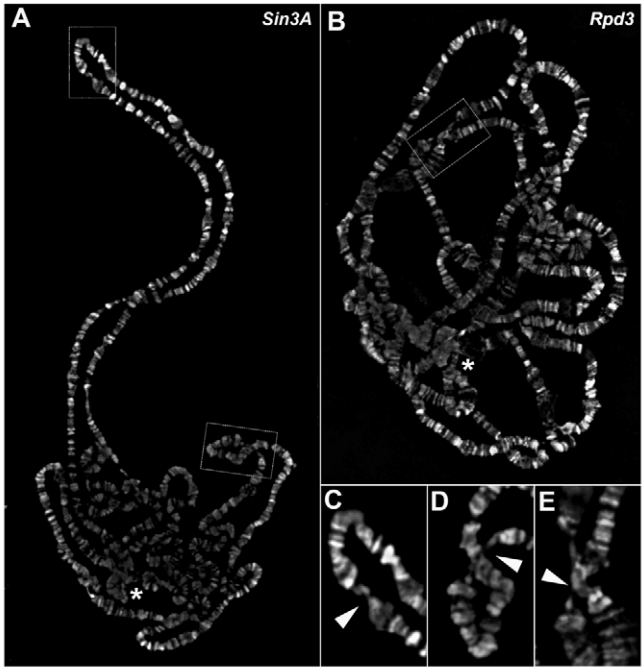

F

Genotypes	Telomere Fusion Score 1	2	3	4	5	*P*-value	*n*
Df(1)yw	37	14	1	0	0	N/A	52
eyGAL4/UAS-Sin3A-RNAi	1	13	30	29	8	<0.001	81
eyGAL4;UAS-Rpd3-RNAi	0	18	35	69	16	<0.001	138
eyGAL4	26	13	5	0	0	<0.7	44
UAS-Sin3A-RNAi	42	11	0	0	0	<0.8	53
UAS-Rpd3-RNAi	46	6	1	0	0	<0.9	53
eyGAL4; UAS-Dicer2	44	10	5	0	0	<0.7	59

Fig. 1. Loss of *Sin3A* and *Rpd3* causes telomeric fusions and the apparent elongation of polytene chromosome ends. DAPI staining of polytene chromosomes from (**A**) *eyGAL4/UAS-Sin3A-RNAi* and (**B**) *eyGAL4;UAS-Rpd3-RNAi* larvae. Asterisks indicate the chromocenter. (**C**–**E**) Higher magnification images of telomere end-to-end fusions of the framed white boxes in A and B. Arrowheads point to both telomere fusion and elongation events. (**F**) Distribution of polytene chromosome telomere fusions for *Sin3A* and *Rpd3* RNAi larvae is based on the number of fused interphase polytene chromosome telomeres scored. Class 1 corresponds to zero fusions, 2 to two telomeres fused, 3 to three telomeres fused, 4 to four telomeres fused and 5 to five telomeres fused (supplementary material Fig. S3). For each genotype tested the statistical significance (*P* value) of the telomere fusion defect was calculated and compared with the telomere fusion distribution observed in the *Df(1)yw* wild type line. The presence of class 2 and 3 fusions in the *Df(1)yw* wild-type line is mostly due to the variability in chromosome spreading preparations, which causes some telomeres to overlap or fall very close.

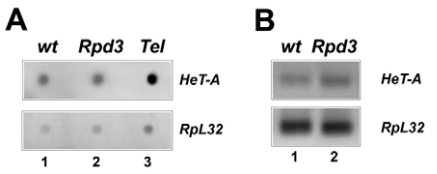

Fig. 2. Telomere fusion in *Rpd3* RNAi lines are not due to an increase in the number of *HeT-A* repeats or of *HeT-A* transcription. (**A**) The amount of *HeT-A* sequences was measured by dot blot using a radiolabeled *HeT-A* probe hybridized to genomic DNA extracted from wild-type (wt; 1), *Rpd3* RNAi (2) and *Tel* mutant (3) salivary glands. A radiolabeled RpL32 probe was used as a loading control. (**B**) *HeT-A* transcription was evaluated by RT-PCR on total RNA derived from wild-type (1) and *Rpd3* RNAi (2) salivary glands. Primers amplifying the ribosomal protein RpL32 were used to normalize the RT-PCR data.

homeostasis, we decided to focus our telomere fusion characterization only on the *Rpd3*-encoded catalytic subunit.

Abnormal telomere elongation and chromosome-end fusions have been observed in *Drosophila* polytene chromosomes as consequence of mutations in the HP1-encoding *Su(var)205* gene and the *Telomere elongation* (*Tel*) gene (Perrini et al., 2004; Siriaco et al., 2002). Telomeres of polytene chromosomes are characterized by the presence of three distinct chromatin domains: the telomere-associated sequences (TASs), the terminal tract of the HTT retrotransposons (*HeT-A*, *TART* and *TAHRE*) and the cap, the most-terminal region that is associated with capping proteins that bind independently of the DNA sequence (Andreyeva et al., 2005; Cenci et al., 2005). In both *Su(var)205* and *Tel* mutants, elongated telomeres result from an increase in *HeT-A* and *TART* elements in the HTT domain. It has been hypothesized that the presence of many tandemly arranged copies of telomeric retrotransposons on long polytene telomeres can increase the likelihood of recombination between telomeric sequences leading to telomere–telomere attachments (Cenci et al., 2005; Perrini et al., 2004; Siriaco et al., 2002).

To ascertain whether the apparent telomere elongation and fusions upon *Rpd3* RNAi were caused by an increase in the amount of telomeric retrotransposable elements at chromosome ends, we conducted classic fluorescent in situ hybridization (FISH) analysis using *HeT-A*, *TART* and *TAHRE* sequences as probes. This analysis revealed that the levels of *HeT-A* (supplementary material Fig. S4A–C), *TART* (supplementary material Fig. S4D–F) and *TAHRE* (supplementary material Fig. S4G–I) sequences were very similar in wild-type telomeres and *Rpd3* RNAi fused telomeres. These results were also confirmed by dot-blot analysis conducted on genomic DNA from *Rpd3* RNAi and *Tel* mutant larval salivary glands. As expected, the dot-blot analysis revealed a significant increase of telomeric genomic DNA *HeT-A* sequences in *Tel* mutants but not upon *Rpd3* RNAi, when compared with wild type (Fig. 2A). Furthermore, because Rpd3 plays a key role in transcription repression (De Rubertis et al., 1996; Pile and Wassarman, 2000; Rundlett et al., 1996), we checked whether *Rpd3* knockdown would affect transcription of telomeric retrotransposons. RT-PCR on RNA samples extracted from salivary glands of wild-type and *Rpd3* RNAi larvae did not show any significant difference in transcription of *HeT-A* sequences (Fig. 2B). Collectively, our data indicate that, unlike for *Tel* and *Su(var)205*, upon *Rpd3* RNAi telomeres are not longer than wild-type, suggesting that the ‘apparently elongated telomeres’ *Rpd3* RNAi phenotype is due to changes in chromatin condensation.

Loss of *Rpd3* affects histone acetylation at telomeres

To assess whether the apparent elongation and fusion phenotypes of the telomere tip upon *Rpd3* RNAi were linked to chromatin condensation changes underlying telomeric histone acetylation defects, we performed immunofluorescence analysis on wild-type and *Rpd3* RNAi chromosomes using antibodies directed against acetylated histones H3 and H4 (AcH3 and AcH4; specifically recognizing K9 and K14 histone H3 acetylations and K5, K8, K12 and K16 histone H4 acetylations), which represent the main histone targets of Rpd3 (Kadosh and Struhl, 1998). Interestingly, loss of *Rpd3* caused a substantial increase in the global levels of both acetylated H3 and H4 histones on polytene chromosomes (Fig. 3A–D), without affecting chromatin loading or expression of non-acetylated histones (supplementary material Fig. S5). Furthermore, western blot analysis on chromatin extracts derived from salivary gland cells, confirmed that chromosomes are loaded with higher levels of both acetylated histones H3 and H4 upon *Rpd3* knockdown when compared with that on wild-type chromosomes (Fig. 3E,F).

Remarkably, upon *Rpd3* RNAi high-magnification images of telomeres immunostained for AcH3 and AcH4, revealed that, whereas the levels of histone H3 acetylation staining slightly increased, the levels and extension of histone H4 acetylation were greatly reduced (Fig. 3B′,D′, white arrowhead and double-arrowed bar). To confirm these findings we measured the levels of histone acetylation specifically associated with telomeric *HeT-A*. To this aim, we optimized a chromatin immunoprecipitation (ChIP) technique on chromatin isolated from salivary glands using the telomere-associated protein HP2 (Fig. 4A). As expected, using antibodies directed against AcH3 and AcH4 we found a substantial increase in *HeT-A*-associated histone H3 acetylation upon *Rpd3* RNAi with respect to that in wild type (Fig. 3G,H, lanes 2 and 6). By contrast, the histone H4 acetylation associated with *HeT-A* sequences was dramatically reduced (Fig. 3G,H, lanes 3 and 7) when compared with that in wild type. These ChIP data are consistent with our immunostaining results and collectively indicate that *Rpd3* RNAi has different effects on histone acetylation at telomeres.

In male polytene chromosomes histone H4 lysine 16 acetylation (AcH4K16) specifically and exclusively localizes to the X chromosome (Gelbart et al., 2009) and is excluded from the male X telomere tip (Fig. 5A, white arrowhead). In *Rpd3*-knockdown polytene chromosomes AcH4K16 is still excluded from X chromosome ends but this loss of localization seems much wider than that for wild-type X chromosome tips (Fig. 5B,C, double-arrowed bar). Interestingly, ectopic AcH4K16 localization starts to appear on some autosomal chromatin loci (Fig. 5B,C, green arrowheads), probably as a consequence of loss of global Rpd3 histone deacetylase activity. ChIP analysis also confirmed a marked reduction of AcH4K16 on *HeT-A* telomeric sequences upon *Rpd3* RNAi (Fig. 5D,E). Taken together, our analyses on histone acetylation suggest that *Rpd3* knockdown causes a significant increase of global H3 and H4 histone acetylation. However, although histone H3 acetylation levels are higher also within telomeric sequences upon *Rpd3* RNAi, acetylation of histone H4 (including that at K16) appeared substantially and specifically decreased at the level of HTT sequences.

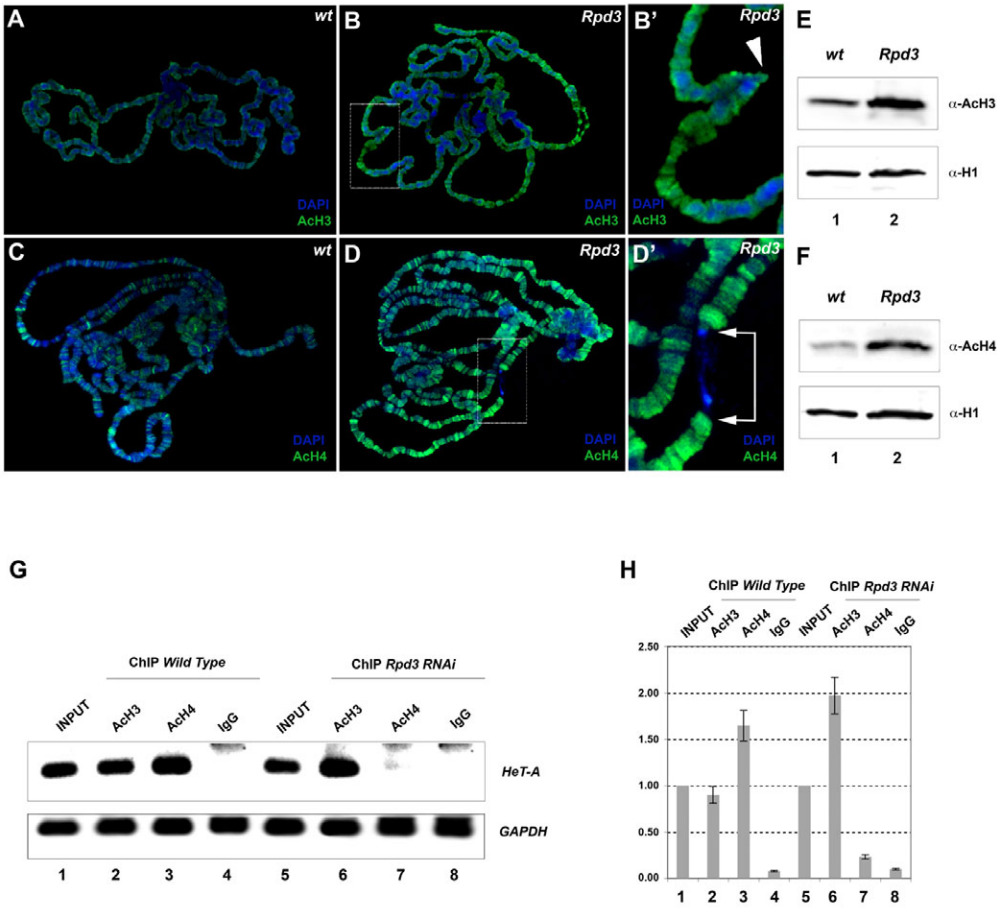

Fig. 3. *Rpd3* knockdown affects global and telomeric histone H3 and H4 acetylation. Immunofluorescence analysis on (**A**,**C**) wild-type (wt) and (**B**,**D**) *Rpd3* RNAi polytene chromosomes using antibodies recognizing (A,B,B′) histone H3 and (C,D,D′) H4 acetylations (histone H3 acetylations on K9 and K14 and histone H4 acetylations on K5, K8, K12 and K16). (B′,D′) A close-up of the framed white areas in B and D, respectively, highlights changes in the levels of histone H3 and H4 acetylations in *Rpd3* RNAi telomere fusions (white arrowhead and double-arrowed bar). (**E**,**F**) Western blot analysis of histone H3 and H4 acetylation on chromatin protein extracts derived from wild-type and *Rpd3* RNAi salivary glands. Chromatin protein loading was normalized with an antibody recognizing the linker histone H1. (**G**) ChIP analysis was performed on chromatin extracted from wild-type and *Rpd3* RNAi salivary glands and was immunoprecipitated using antibodies against acetylated H3 and H4. Chromatin immunoprecipitation was performed in triplicates and analyzed by PCR using specific primers for the telomeric *HeT-A* sequences and *GAPDH* as a control for non-telomeric targets. (**H**) Quantification of the anti-AcH3 and anti-AcH4 antibody ChIP experiments, relative to 'input' chromatin.

Rpd3 regulates heterochromatin marks on polytene telomeres

To investigate whether the marked decrease in histone H4 acetylation levels associated with telomeric *HeT-A* upon *Rpd3* RNAi affected other telomere-associated epigenetic modifications, we analyzed the distribution of three common heterochromatin histone modifications: trimethlyated histone H4K20 (trimeH4K20), trimethlyated histone H3K9 (trimeH3K9) and trimethlyated histone H3K27 (trimeH3K27). Normally, trimeH4K20 is found in the heterochromatic chromocenter and in numerous euchromatic bands (Fig. 5H) (Ebert et al., 2006), trimeH3K27 is associated with the chromocenter, telomeric TASs and a subset of about ~100 bands (Fig. 5J) (Andreyeva et al., 2005), whereas trimeH3K9 localizes at pericentric heterochromatin, at telomeres and at a number of sites along chromosome arms (Fig. 5F). We found that *Rpd3* knockdown decreased the global localization of all three modified histones on polytene chromosome arms (Fig. 5G,I,K) when compared with wild type. However, although the levels of trimeH4K20 and trimeH3K27 were reduced also at telomeres upon *Rpd3* RNAi (Fig. 5I′,K′, white arrowheads), the amount of H3K9 trimethylation increased in *Rpd3*-knockdown telomeres (Fig. 5G′, white arrowhead). As it has been previously shown trimeH3K9 localizes at the telomeric HTT domain (Andreyeva et al., 2005) and HTT telomeric sequences are not amplified in telomeres upon *Rpd3* RNAi (Fig. 2), the observed trimeH3K9 accumulation combined with the reduced trimeH3K27 levels could reflect a change in heterochromatin structure in telomeres upon *Rpd3* RNAi.

As we were unable to find ChIP primers specific for TAS sequences (data not shown), we conducted FISH analysis in order to obtain some low-resolution information about global chromatin organization of TAS in both wild-type and telomeres and upon *Rpd3* RNAi. The FISH data indicate that, whereas in wild-type strains the TASs showed a wide punctuated localization at telomeres (Fig. 6A, double arrowed bars in 6A′ and 6A″), in *Rpd3*-knockdown TAS FISH signals on telomeres were slightly more compacted (Fig. 6B, double arrowed bar on the 3L–X chromosome fusion and white bar on the 2L unfused chromosome in B′). This apparent slightly compacted TAS localization pattern in *Rpd3*-knockdown polytene chromosomes was not due to a reduction of TAS copies, as their number did not appear different from that observed in the w^{1118} control strain (data not shown). Thus, it is probably a

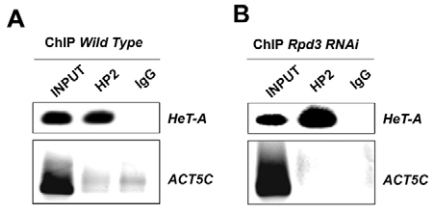

Fig. 4. ChIP on salivary gland polytene chromatin specifically detects *HeT-A* sequences. ChIP analysis was performed on chromatin extracted from wild-type and *Rpd3* RNAi salivary glands and immunoprecipitated using an antibody against HP2. Chromatin immunoprecipitation was analyzed by PCR using specific primers for the telomeric *HeT-A* sequences and *ACT5C* as a control for non-telomeric targets.

consequence of a change in chromatin compaction that affects the organization of the sequences and/or probe accessibility to its specific complementary sequence.

Loss of Rpd3 causes an accumulation of telomeric HP2

It is widely accepted that trimeH3K9 at chromosome ends is a key conserved mark for a proper localization of telomeric capping proteins (Schoeftner and Blasco, 2009). Thus, we wanted to verify whether accumulation of trimeH3K9 in telomeres upon *Rpd3* RNAi influenced the localization of proteins known to have essential functions in *Drosophila* telomere maintenance. Immunofluorescence using antibodies directed against specific telomere capping proteins showed that *Rpd3* knockdown did not affect the localization or abundance of HOAP (encoded by the *caravaggio* gene) (Fig. 7A–C,J) (Cenci et al., 2003; Shareef et al., 2001), HP1 (Fig. 7D–F,J) (Fanti et al., 1998; Perrini et al., 2004) or Woc (Fig. 7G-I,J) (Raffa et al., 2005) in either fused or non-fused telomeres, indicating that capping proteins localize normally upon *Rpd3* RNAi. The fact the HP1 localization and function is not affected as consequence of changes in telomeric levels of trimeH3K9 strengthens previous observations that the interaction between the HP1 chromodomain and trimeH3K9 is not required for the capping function of HP1 (Ebert et al., 2004; Perrini et al., 2004).

Because specific histone modifications are crucial for the localization of heterochromatin proteins, we sought to determine whether alterations in both AcH4 and trimeH3K9 caused by loss of *Rpd3* influenced the distributions of heterochromatin proteins that, like HP1, associate with chromosome ends in *Drosophila*. We therefore analyzed the telomere localization pattern of HP2, an HP1-interacting factor with a role in the structural organization of chromosomes and in heterochromatin-induced gene silencing (Shaffer et al., 2006). In polytene chromosomes HP2 localizes at the chromocenter, at distinct chromosomal bands and at the cap of telomeres (Andreyeva et al., 2005; Shaffer et al., 2006). However, unlike HP1, HP2 is not a capping protein and is not required to prevent chromosome fusions (Shaffer et al., 2006). Surprisingly, immunofluorescence (Fig. 5L–M′; Fig. 7J) and ChIP (Fig. 4B) analyses revealed a striking accumulation of HP2 at fused and non-fused telomeres upon *Rpd3* RNAi, although the localization of HP2 at the chromocenter and other chromosomal regions remained indistinguishable from wild type (data not shown).

Discussion

We have identified the Rpd3–Sin3A histone deacetylase complex as a factor establishing proper chromatin structure of *Drosophila* telomeres. Strikingly, loss of Rpd3 dramatically affected the organization of polytene chromosome ends resulting in telomere prone to fusions. Interestingly, the observations that upon *Rpd3* RNAi telomeric fusions are not seen in mitotic cells and that

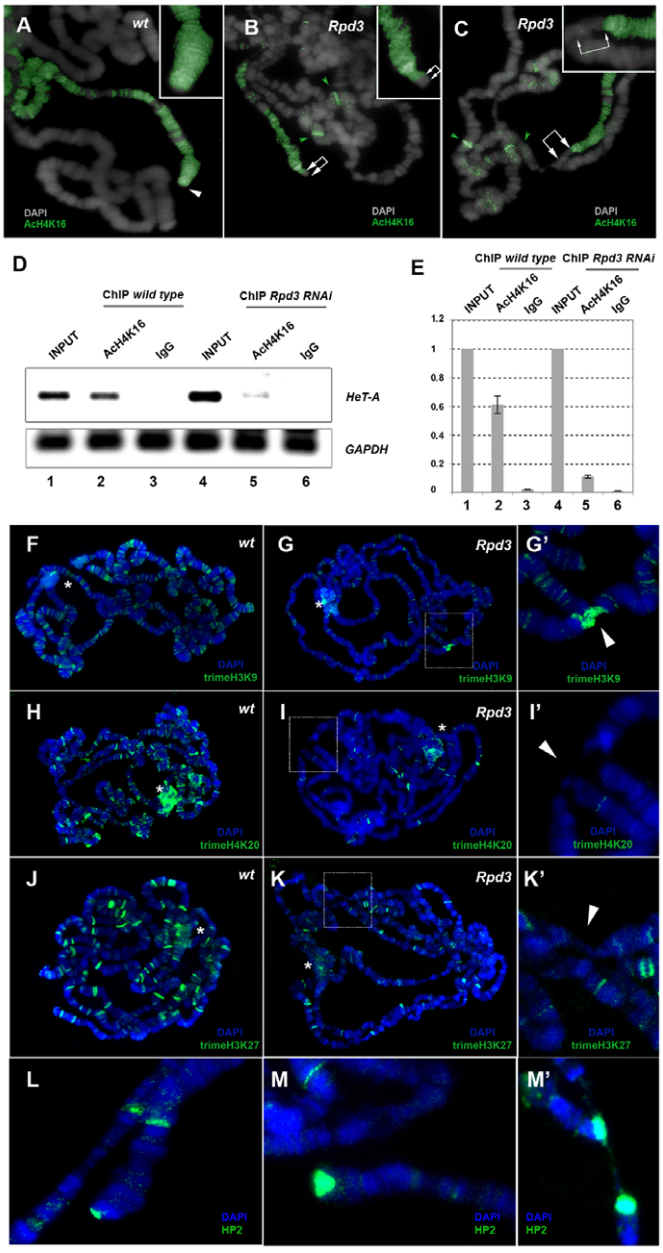

Fig. 5. Loss of *Rpd3* alters site-specific histone H4K16 acetylation and causes an accumulation of trimeH3K9 and HP2 at telomeres. Immunofluorescence analysis with an antibody recognizing H4K16 acetylation (AcH4K16) on wild-type (wt) (**A**) and not-fused (**B**) or fused (**C**) *Rpd3* RNAi male polytene chromosomes. The inserts show a magnified image of the male X telomere tips. The white arrowhead and the double-arrowed bar indicate changes in the levels of AcH4K16 in telomere tips upon *Rpd3* RNAi. The green arrowheads indicate the appearance of non-specific autosomal H4K16 acetylated chromatin domains on chromosomes upon *Rpd3* RNAi. (**D**) ChIP analysis was performed using antibodies against acetylated H4K16 (AcH4K16) to immunoprecipitate chromatin extracted from wild-type and *Rpd3* RNAi salivary glands. Chromatin immunoprecipitation was performed in triplicates and analyzed by PCR using specific primers for the telomeric *HeT-A* sequences and *GAPDH* as a control for non-telomeric targets. (**E**) Quantification of the anti-AcH4K16 antibody ChIP experiment, relative to input chromatin. Immunofluorescence on (**F**,**H**,**J**) wild-type and (**G**,**I**,**K**) *Rpd3* RNAi polytene chromosomes using antibodies recognizing trimethylated histone H3K9 (trimeH3K9), trimethylatated H4K20 (trimeH4K20) and trimethylated H3K27 (trimeH3K27). (**G′**,**I′**,**K′**) A magnified image of the white-boxed areas in G, I and K, respectively, shows in the detail the changes in trimeH3K9, trimeH4K20 and trimeH3K27 histone modifications occurring at the telomere fusions sites. The asterisk indicates the chromocenter and the white arrowheads point to telomere fusions. Immunofluorescence staining with the anti-HP2 antibody on (**L**) wild-type and *Rpd3* RNAi mutant polytene not-fused (**M**) and fused (**M′**) chromosome ends shows that the HP2 protein accumulates in telomeres upon *Rpd3*-knockdown.

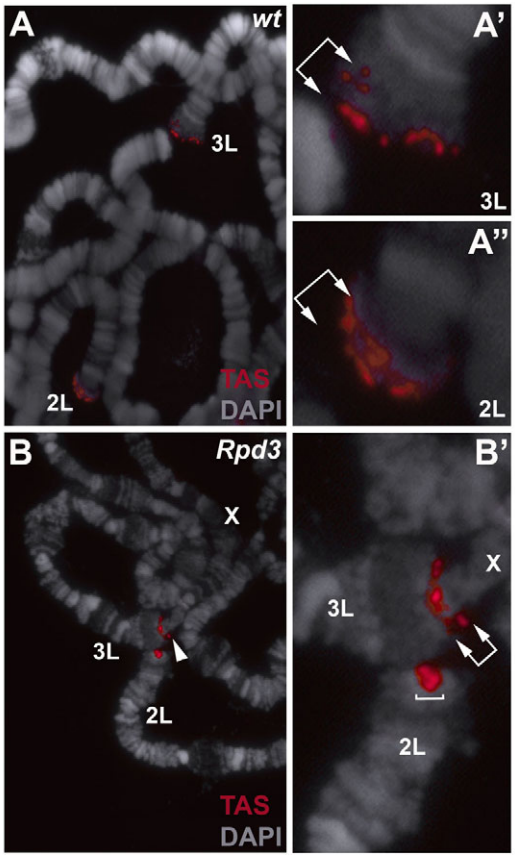

Fig. 6. Chromatin organization of TASs in *Rpd3* RNAi polytene chromosome telomeres. FISH analysis of TASs in wild-type (wt) (**A**) and *Rpd3* RNAi (**B**) unfused and fused telomeres. Arrowhead point to chromosome fusion. Wild-type TASs show a wide and punctuated localization at telomeres, whereas upon *Rpd3* knockdown TASs present a slight but highly penetrant (100%; *n*=50) reduction in the extension of the FISH signal along both chromosome axes, probably reflecting a change in chromatin compaction following loss of *Rpd3* or probe accessibility. (**A′**,**A″**,**B′**) Magnified images of the TAS FISH signals shown in A and B, respectively. Double arrowed bars show the extension of FISH signals along the telomere–centromere axis. Note that extension of TAS FISH signals in *Rpd3* RNAi telomeres is slightly reduced when compared with that in wild type. The white bar indicates an area with a substantial reduction of FISH signal along the width of an unfused *Rpd3*-knockdown 2L telomere.

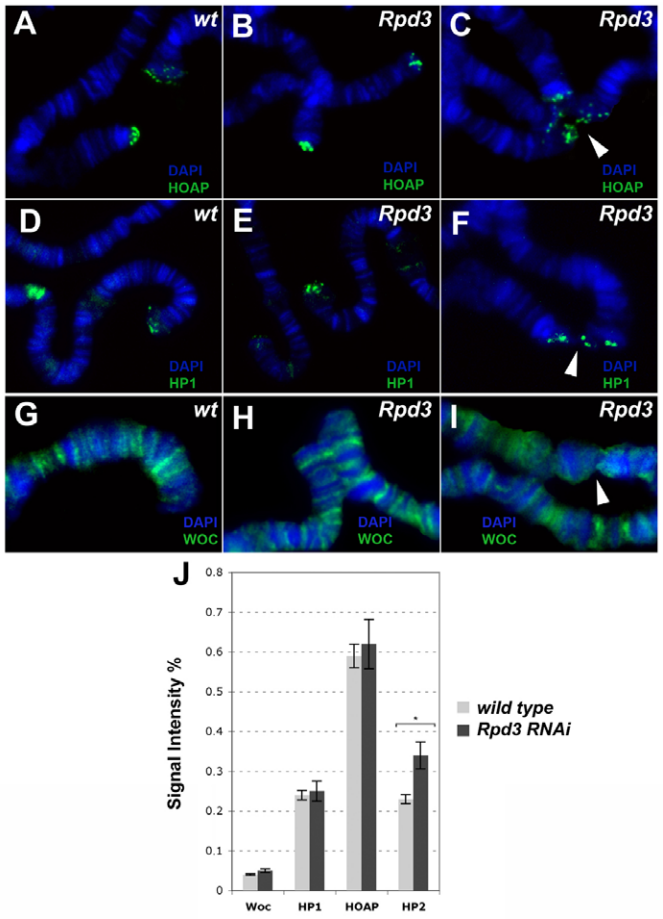

Fig. 7. Localization and loading of telomere capping factors in *Rpd3* RNAi polytene chromosome telomeres. (**A**–**C**) Immunostaining of HOAP, (**D**–**F**) HP1 and (**G**–**I**) Woc in (A,D,G) wild-type (wt) and *Rpd3* RNAi (B,E,H) non-fused and (C,F,I) fused chromosomes. White arrowheads point to telomere fusions. (**J**) Quantification of telomere localization of capping proteins (Woc, HP1 and HOAP) and HP2 on wild-type and *Rpd3* RNAi chromosome-ends. Note that only the HP2 percentage of signal intensity is significantly higher (*P<0.001, χ^2 test) on mutant telomeres with respect to that on wild-type chromosome ends (asterisk).

telomere capping proteins localize normally further suggest that the activity of Rpd3 is not required for chromosome end protection.

Fused polytene telomeres have been always associated with an increase in HTT copies. Surprisingly, our FISH analysis, along with dot-blot results, clearly indicated that in *Rpd3*-knockdown telomeres the amount of the *HeT-A*, *TART* and *TAHRE* elements remained as high as in wild type. The apparent telomere elongation we observed upon *Rpd3* RNAi probably reflects a change in telomere chromatin condensation in *Rpd3* mutants, underlying changes in histone acetylation. As a result of this change in telomere chromatin condensation, *Rpd3* mutants possess telomere tips that appear ‘longer’ than usual by DAPI staining.

A combination of immunostaining and ChIP data indicated that loss of *Rpd3* by RNAi leads to profound global, as well as telomeric, chromatin epigenetic changes. Upon specific *Rpd3* RNAi telomere epigenetic changes included a decrease in H4 acetylation, including H4K16Ac, and an increase of trimeH3K9 at the level of telomere tips. Moreover, the HP2 protein, which normally binds to the telomere cap, was highly enriched upon *Rpd3* RNAi. Because we were unable to perform ChIP on TAS sequences, we could not directly assess whether the epigenetic changes induced by *Rpd3* RNAi also affected TAS sequences. Nevertheless, the apparent slight compaction of TAS organization detected by FISH in polytene chromosomes upon *Rpd3* RNAi suggests that loss of *Rpd3* affects the structural chromatin organization of this region.

The question of how the accumulation of HP2 on telomeric chromatin with reduced H4Ac and increased trimeH3K9, is linked to the fusion of telomeres upon *Rpd3* RNAi still remains open. One intriguing possibility is that an overload of HP2 drives excessive heterochromatization at chromosome ends upon *Rpd3* RNAi, inducing telomeric stickiness reminiscent of chromocenter heterochromatin coalescence. Alternatively, an excess of

heterochromatization might also impair telomere replication leading to stalled replication forks, which are known to cause fusigenic telomeres (Ferreira et al., 2004).

In conclusion, our work provides an important insight into the epigenetic determination of telomere chromatin organization in higher eukaryotes. As polytene chromosomes are known to be useful cytogenetic tools to address the question of structural and functional organization of telomeres in *Drosophila*, our results might represent a foothold for further studies to understand the interplay existing between histone acetylation and deacetylation events and telomere homeostasis.

Materials and Methods

Drosophila stocks and genetic crosses

Flies were raised on cornmeal-yeast-agar medium containing Tegosept. *Drosophila* RNAi strains and w^{1118};*P[UAS-dicer2, w*$^{+}$*]* were obtained from the Vienna *Drosophila* RNAi Center (http://stockcenter.vdrc.at/control/main).

To monitor the effects of *Sin3A* RNAi and *Rpd3* RNAi on polytene chromosomes structure, larvae were generated by crossing homozygous *yw, P[w*$^{+}$*, eyGAL4]* virgins (Hazelett et al., 1998) with homozygous *UAS-Sin3A-RNAi* (VDRC 10808) or heterozygous *UAS-Rpd3-RNAi/T(2:3) CyO, Hu, Tb* flies, recognizing the larvae of interest by the absence of the dominant marker Tb. The *UAS-Rpd3-RNAi/T(2:3) CyO, Hu, Tb* stock was obtained from *Rpd3* RNAi strain VDRC 30599 balanced with *T(2:3) CyO, Hu, Tb*. The *eyGAL4* driver, beside its specific expression in the eye discs has also a leaky expression in salivary glands, but not in neuroblasts, allowing the analysis of *Rpd3* RNAi on polytene chromosomes (Corona et al., 2007). For the analysis of mitotic chromosomes, heterozygous *UAS-Rpd3-RNAi/T(2:3) CyO, Hu, Tb* and homozygous *UAS-Sin3A-RNAi* males were crossed with *daGAL4* virgins (Corona et al., 2007). The *daGAL4* driver is expressed ubiquitously in embryos and continues its expression in many other larval tissues, including the brain (neuroblasts), allowing the analysis of *Rpd3* RNAi files on mitotic chromosomes (Corona et al., 2007).

Analysis of polytene and mitotic chromosomes

Df[yw], *eyGAL4/UAS-Sin3A-RNAi* and *eyGAL4;UAS-Rpd3-RNAi* mutant polytene chromosomes were prepared from third-instar larvae grown at 20°C. For single staining, polytene chromosome were processed as described previously (Burgio et al., 2008; Raffa et al., 2005). The primary antibodies used for immunostainings include rabbit antibodies against Sin3A (Pile and Wassarman, 2000), Rpd3 (Pile and Wassarman, 2000), acetylated histone H3 and H4 (Upstate; specifically recognizing histone H3 acetylations on K9 and K14 and histone H4 acetylations on K5, K8, K12 and K16), acetylated lysine 16 of histone H4 (Active Motif), trimethylated lysine 9 of H3 and trimethylated lysine 20 of H4 (UBI) (Schotta et al., 2004), a mouse antibody against trimethylated lysine 27 of H3 (Abcam) and antibodies against HOAP, HP1 and Woc (Raffa et al., 2005). For fluorescence in situ hybridization (FISH) we used the pSC-23Zn plasmid containing the 23ZnORF of HeT-A and the pOR-i4-2 plasmid corresponding to ORF1 e ORF2 of TART (Perrini et al., 2004). *TAHRE* probes were obtained from PCR reactions on genomic DNA using T1 and T2 specific primers (Shpiz et al., 2007). Chromosome 2L TAS probes were obtained by PCRs on genomic DNA using the following primers couple: 2L TAS 1F (5′-GACAATGCACGACAGAGGAA-3′) and 2L TAS 1R (5′-CTCTCGCATACG-CGATCATA-3′). Probes were directly labeled with biotine-16-dUTP (Roche) and FISH was performed as previously described (Perrini et al., 2004). Mitotic metaphase chromosomes from larval brain cells were obtained as previously reported (Raffa et al., 2005). Images were captured with a DC360 FX camera on a Leica DM 4000B microscope. Quantitative densitometric analysis was performed using the LAS (Leica) software. Images were elaborated with the Adobe PhotoShop CS software.

Protein extracts and western blotting analysis

Salivary glands total protein extracts from the *Df[yw]*, *eyGAL4/UAS-Sin3A-RNAi* and *eyGAL4;UAS-Rpd3-RNAi* mutant third-instar larvae were obtained dissecting the glands in 0.7% NaCl, following vortexing in of RIPA buffer (2 µl for each pair of glands; 1% NP40, 0.5% sodium deoxicolate, 0.1% SDS in PBS). The homogenate was centrifuged at 20,000 ***g*** for 30 min and the supernatant was flash frozen in liquid nitrogen and stored at –80°C (Burgio et al., 2008). Salivary glands chromatin extracts were prepared as described previously (Corona et al., 2007). Proteins were fractionated by SDS-PAGE and analyzed by protein blotting using rabbit antibodies against Sin3A and Rpd3 (Pile and Wassarman, 2000), acetylated histone H3 and H4 (Upstate) and against histone H1 (Corona et al., 2007). The chemiluminescent HRP-conjugated secondary antibodies were developed using the Super Signal West Femto substrate (Pierce) and acquired with the ChemiDoc XRS imager (Bio-Rad).

RT-PCR and dot-blotting of *HeT-A* sequences

For RT-PCR, total RNA was isolated from *Df[yw]* and *eyGAL4;UAS-Rpd3-RNAi* larval salivary glands by using TRIzol (Invitrogen). The total RNA was reverse transcribed by using the oligo d(T) GeneAmp RNA PCR kit (Applied Biosystems). The first-strand cDNA was used as a template for PCR reactions with primers specific for *HeT-A* and *RpL32* (HeT-A forward, 5′-GGCAGCATATTAGCGC-GTACA-3′ and HeT-A reverse, 5′-TTTGCCGCCAGCTTTTGT-3′; RpL32 forward, 5′-CAAGAAGTTCCTGGTGCACAAC-3′ and RpL32 reverse, 5′-AAACGCGGTTCTGCATGAG-3′) (Perrini et al., 2004). To exclude amplification of genomic DNA contamination present in our RNA samples, we always included a mock RT-PCR reaction lacking the reverse transcriptase as a negative control. Agarose gels were stained with ethidium bromide and images were acquired with the ChemiDoc XRS Imager (Bio-Rad). For dot blots, genomic DNA from *Df[yw]*, *eyGAL4;UAS-Rpd3-RNAi* and *Tel* mutant larval salivary glands was obtained by using classical phenol-chloroform–isoamyl alcohol extraction and then cross-linked on Hybond-N+ membrane (Amersham). A PCR-amplified *HeT-A* probe was obtained using the pSC-23Zn plasmid as a template and the primers specific for *HeT-A* used for the RT-PCR described above (Perrini et al., 2004). The *RpL32* probe was obtained from cDNA retro-transcribed from the total RNA of salivary glands and was PCR-amplified with the primers used for RT-PCR described above (Perrini et al., 2004). Membranes were hybridized with *HeT-A* and *RpL32* probes labeled with the Random Primed DNA Labeling kit (Roche). Radioactive signals were acquired with the Personal Molecular Imager (BioRad).

ChIP

Chromatin was extracted from 40 pairs of *Df[yw]* and *eyGAL4;UAS-Rpd3-RNAi* salivary glands and ChIP was conducted with 2 µg of anti-AcH3 and anti-AcH4 antibodies (Upstate; specifically recognizing histone H3 acetylations on K9 and K14 and histone H4 acetylations on K5, K8, K12 and K16), anti-H4K16Ac (Active Motif), and 1 µg of anti HP2, as described previously (Larschan et al., 2007), adapting reaction volumes to the small chromatin sample. In all experiments presented the ‘Input’ chromatin corresponds to 15% of chromatin used for the ChIP. Input and immunoprecipitated DNA fragments (PCR purification kit; Quiagen) were amplified by using the GenomePlex complete whole genome amplification (WGA) kit (SIGMA) and then primers specific for *HeT-A* (HeT-A forward, 5′-GGCAGCATATT-AGCGCGTACA-3′ and HeT-A reverse, 5′-TTTGCCGCCAGCTTTTGT-3′); *ACT5C* (ACT5C forward, 5′-CACGGTATCGTGACCAACTG-3′ and ACT5C reverse, 5′-GCCATCTCCTGCTCAAAGTC-3′) or *GAPDH* (GAPDH forward, 5′-TACTAGCGGTTTTACGGGCG-3′ and GAPDH reverse, 5′-TCGAACAGGAGG-AGCAGAGAGCGA-3′) were used for PCR or RT-PCR amplification (Perrini et al., 2004). PCR products were analyzed on agarose gels stained with ethidium bromide and images were acquired with ChemiDoc XRS imager (Bio-Rad). Quantification of bands was performed with Quantity One software (Bio-Rad).

We thank the Bloomington and VDRC Stock Center for the *Drosophila* strains used in this work. We are grateful to Lori Pile for providing the anti-Sin3A and anti-Rpd3 antibodies, Thomas Jenuwein for the anti-trimeH3K9, anti-trimeH3K27 and anti-trimeH4K20 antibodies, Jim Kadonaga for the anti-H1 antibody, Sarah Elgin for the anti-HP2 antibody, Laura Ciapponi for the anti-HOAP antibody, Grazia Raffa for the anti-Woc antibody, Mary-Lou Pardue for the pSC-23Zn plasmid and Sergio Pimpinelli for the pOR-i4-2 plasmid. We also thank S. Rosalia for her inspiring vision of our work. G.B. was supported by a FIRC Fellowship and AMRI by a Telethon Fellowship. This work was supported by grants from MIUR-PRIN and AIRC to G.C. and by Fondazione Telethon, Giovanni Armenise Harvard Foundation, MIUR-FIRB, HFSP, AIRC and EMBO YIP to D.F.V.C.

Supplementary material available online at
http://jcs.biologists.org/cgi/content/full/124/12/2041/DC1

References

Ahringer, J. (2000). NuRD and SIN3 histone deacetylase complexes in development. *Trends Genet.* **16**, 351-356.

Altaf, M., Utley, R. T., Lacoste, N., Tan, S., Briggs, S. D. and Cote, J. (2007). Interplay of chromatin modifiers on a short basic patch of histone H4 tail defines the boundary of telomeric heterochromatin. *Mol. Cell* **28**, 1002-1014.

Andreyeva, E. N., Belyaeva, E. S., Semeshin, V. F., Pokholkova, G. V. and Zhimulev, I. F. (2005). Three distinct chromatin domains in telomere ends of polytene chromosomes in Drosophila melanogaster Tel mutants. *J. Cell Sci.* **118**, 5465-5477.

Blasco, M. A. (2007). The epigenetic regulation of mammalian telomeres. *Nat. Rev. Genet.* **8**, 299-309.

Burgio, G., La Rocca, G., Sala, A., Arancio, W., Di Gesu, D., Collesano, M., Sperling, A. S., Armstrong, J. A., van Heeringen, S. J., Logie, C. et al. (2008). Genetic identification of a network of factors that functionally interact with the nucleosome remodeling ATPase ISWI. *PLoS Genet.* **4**, e1000089.

Cenci, G., Siriaco, G., Raffa, G. D., Kellum, R. and Gatti, M. (2003). The Drosophila HOAP protein is required for telomere capping. *Nat. Cell Biol.* **5**, 82-84.

Cenci, G., Ciapponi, L. and Gatti, M. (2005). The mechanism of telomere protection: a comparison between Drosophila and humans. *Chromosoma* **114**, 135-145.

Ciapponi, L. and Cenci, G. (2008). Telomere capping and cellular checkpoints: clues from fruit flies. *Cytogenet. Genome Res.* **122**, 365-373.
Corona, D. F., Siriaco, G., Armstrong, J. A., Snarskaya, N., McClymont, S. A., Scott, M. P. and Tamkun, J. W. (2007). ISWI regulates higher-order chromatin structure and histone H1 assembly in vivo. *PLoS Biol.* **5**, e232.
De Lange, T. (2005). Telomere-related genome instability in cancer. *Cold Spring Harb. Symp. Quant. Biol.* **70**, 197-204.
De Rubertis, F., Kadosh, D., Henchoz, S., Pauli, D., Reuter, G., Struhl, K. and Spierer, P. (1996). The histone deacetylase RPD3 counteracts genomic silencing in Drosophila and yeast. *Nature* **384**, 589-591.
Dietzl, G., Chen, D., Schnorrer, F., Su, K. C., Barinova, Y., Fellner, M., Gasser, B., Kinsey, K., Oppel, S., Scheiblauer, S. et al. (2007). A genome-wide transgenic RNAi library for conditional gene inactivation in Drosophila. *Nature* **448**, 151-156.
Ebert, A., Schotta, G., Lein, S., Kubicek, S., Krauss, V., Jenuwein, T. and Reuter, G. (2004). Su(var) genes regulate the balance between euchromatin and heterochromatin in Drosophila. *Genes Dev.* **18**, 2973-2983.
Ebert, A., Lein, S., Schotta, G. and Reuter, G. (2006). Histone modification and the control of heterochromatic gene silencing in Drosophila. *Chromosome Res.* **14**, 377-392.
Fanti, L., Giovinazzo, G., Berloco, M. and Pimpinelli, S. (1998). The heterochromatin protein 1 prevents telomere fusions in Drosophila. *Mol. Cell* **2**, 527-538.
Ferreira, M. G., Miller, K. M. and Cooper, J. P. (2004). Indecent exposure: when telomeres become uncapped. *Mol. Cell* **13**, 7-18.
Gelbart, M. E., Larschan, E., Peng, S., Park, P. J. and Kuroda, M. I. (2009). Drosophila MSL complex globally acetylates H4K16 on the male X chromosome for dosage compensation. *Nat. Struct. Mol. Biol.* **16**, 825-832.
Hazelett, D. J., Bourouis, M., Walldorf, U. and Treisman, J. E. (1998). decapentaplegic and wingless are regulated by eyes absent and eyegone and interact to direct the pattern of retinal differentiation in the eye disc. *Development* **125**, 3741-3751.
Johansen, K. M., Johansen, J., Jin, Y., Walker, D. L., Wang, D. and Wang, Y. (1999). Chromatin structure and nuclear remodeling. *Crit. Rev. Eukaryot. Gene Expr.* **9**, 267-277.
Kadosh, D. and Struhl, K. (1998). Targeted recruitment of the Sin3-Rpd3 histone deacetylase complex generates a highly localized domain of repressed chromatin in vivo. *Mol. Cell. Biol.* **18**, 5121-5127.
Larschan, E., Alekseyenko, A. A., Gortchakov, A. A., Peng, S., Li, B., Yang, P., Workman, J. L., Park, P. J. and Kuroda, M. I. (2007). MSL complex is attracted to genes marked by H3K36 trimethylation using a sequence-independent mechanism. *Mol. Cell* **28**, 121-133.
Mason, J. M., Frydrychova, R. C. and Biessmann, H. (2008). Drosophila telomeres: an exception providing new insights. *BioEssays* **30**, 25-37.
Nugent, C. I. and Lundblad, V. (1998). The telomerase reverse transcriptase: components and regulation. *Genes Dev.* **12**, 1073-1085.
Palm, W. and de Lange, T. (2008). How shelterin protects mammalian telomeres. *Annu. Rev. Genet.* **42**, 301-334.
Perrini, B., Piacentini, L., Fanti, L., Altieri, F., Chichiarelli, S., Berloco, M., Turano, C., Ferraro, A. and Pimpinelli, S. (2004). HP1 controls telomere capping, telomere elongation, and telomere silencing by two different mechanisms in Drosophila. *Mol. Cell* **15**, 467-476.
Pile, L. A. and Wassarman, D. A. (2000). Chromosomal localization links the SIN3-RPD3 complex to the regulation of chromatin condensation, histone acetylation and gene expression. *EMBO J.* **19**, 6131-6140.
Raffa, G. D., Cenci, G., Siriaco, G., Goldberg, M. L. and Gatti, M. (2005). The putative Drosophila transcription factor woc is required to prevent telomeric fusions. *Mol. Cell* **20**, 821-831.
Rashkova, S., Karam, S. E., Kellum, R. and Pardue, M. L. (2002). Gag proteins of the two Drosophila telomeric retrotransposons are targeted to chromosome ends. *J. Cell Biol.* **159**, 397-402.
Rundlett, S. E., Carmen, A. A., Kobayashi, R., Bavykin, S., Turner, B. M. and Grunstein, M. (1996). HDA1 and RPD3 are members of distinct yeast histone deacetylase complexes that regulate silencing and transcription. *Proc. Natl. Acad. Sci. USA* **93**, 14503-14508.
Schoeftner, S. and Blasco, M. A. (2009). A 'higher order' of telomere regulation: telomere heterochromatin and telomeric RNAs. *EMBO J.* **28**, 2323-2336.
Schotta, G., Lachner, M., Sarma, K., Ebert, A., Sengupta, R., Reuter, G., Reinberg, D. and Jenuwein, T. (2004). A silencing pathway to induce H3-K9 and H4-K20 trimethylation at constitutive heterochromatin. *Genes Dev.* **18**, 1251-1262.
Shaffer, C. D., Cenci, G., Thompson, B., Stephens, G. E., Slawson, E. E., Adu-Wusu, K., Gatti, M. and Elgin, S. C. (2006). The large isoform of Drosophila melanogaster heterochromatin protein 2 plays a critical role in gene silencing and chromosome structure. *Genetics* **174**, 1189-1204.
Shareef, M. M., King, C., Damaj, M., Badagu, R., Huang, D. W. and Kellum, R. (2001). Drosophila heterochromatin protein 1 (HP1)/origin recognition complex (ORC) protein is associated with HP1 and ORC and functions in heterochromatin-induced silencing. *Mol. Biol. Cell* **12**, 1671-1685.
Shpiz, S., Kwon, D., Uneva, A., Kim, M., Klenov, M., Rozovsky, Y., Georgiev, P., Savitsky, M. and Kalmykova, A. (2007). Characterization of Drosophila telomeric retroelement TAHRE: transcription, transpositions, and RNAi-based regulation of expression. *Mol. Biol. Evol.* **24**, 2535-2545.
Siriaco, G. M., Cenci, G., Haoudi, A., Champion, L. E., Zhou, C., Gatti, M. and Mason, J. M. (2002). Telomere elongation (Tel), a new mutation in Drosophila melanogaster that produces long telomeres. *Genetics* **160**, 235-245.
Steitz, M. C., Wickenheisser, J. K. and Siegfried, E. (1998). Overexpression of zeste white 3 blocks wingless signaling in the Drosophila embryonic midgut. *Dev. Biol.* **197**, 218-233.
Stephens, G. E., Craig, C. A., Li, Y., Wallrath, L. L. and Elgin, S. C. (2004). Immunofluorescent staining of polytene chromosomes: exploiting genetic tools. *Methods Enzymol.* **376**, 372-393.